SMWD 2023, KTH Royal Institute of Technology, Stockholm, $23^{rd} - 25^{th}May2023$

Structurally Fuselage-Integrated Wide-Scanning Array Antenna

Prabhat Khanal(1), Jian Yang(1), Ruoshan Luo(2), Per Hallander(2), and Mussie Gebretnsae(2)*
(1) Chalmers University of Technology, Gothenburg, Sweden
(2) Saab AB, Sweden

Summary

A low-profile, wide-scanning array antenna of vertical bowtie elements fully integrated with a structurally efficient radome and ribs of an aircraft fuselage is shown in this paper. The array is designed to simultaneously fulfil the electrical requirements of an airborne antenna sensor and the mechanical needs of a load-carrying aircraft fuselage. The 16×16 array of the purposed vertical bowtie element is capable of steering the beam up to ±60° and ±75° with the bandwidth of 20% and 10%, respectively at $\Gamma_{act} \leq -10$ dB. It also showed good stiffness and performed well against the vibration loads of commercial transport aircraft.

1 Introduction

Modern aircraft typically use more than 20 antennas protruding from their fuselage [1]. These exterior antennas affect the aerodynamic performance of the aircraft and increase the aircraft weight that increases fuel consumption and production of harmful gases like CO_2 and NO_x [2]. They are also subject to considerable wear and tear, and could fail due to extremes of environments causing operational delays and increasing maintenance costs [3]. A multi-functional fuselage structure with an integrated array antenna, as shown in Fig. 1a, could be utilized to avoid these antenna protrusions. Aircraft fuselages carry bending moments, shear forces, and torsional loads. Therefore, the fuselage-integrated antenna should be integrated with a structurally efficient load-carrying radome so that they (together) provide the structural integrity necessary for the aircraft fuselage as well as fulfil the RF performance of the antenna sensor. State-of-art structurally fuselage-integrated array antennas have been developed for satellite communication at Ku-band, such as those in [4] and [5] capable of steering beam up to ±45°. In this paper, we present a vertically connected dual-layered capped bowtie array at S-band, structurally integrated with an aircraft fuselage and capable of beam steering up to ±75° with $\Gamma_{act} \leq -10$ dB over the entire mechanical load envelope.

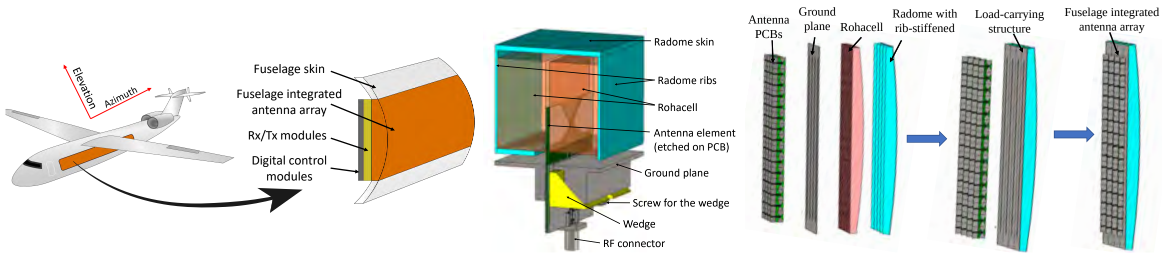

(a) The fuselage integrated array concept **(b)** Unitcell element **(c)** The fuselage integrated array assembly

Figure 1. (a) The fuselage integrated array concept, (b) antenna element unitcell and (c) the fuselage integrated array assembly.

2 Array design

The unitcell of the antenna element with the radome is shown in Fig. 1b. The element consists of a pair of bowties, each located on one of the outermost sides of a three-layered PCB and is excited with a folded balun which is etched on the middle layer of the PCB. The Rohacell dampens the vibrations during flight and prevents PCBs from breaking. The wedges guide the PCBs to align in the correct position during array assembly. The radome is curved in the vertical direction with a radius of curvature which corresponds to that of a medium-range aircraft and is stiffened with transverse ribs. The radome together with the Rohacell and the ground plane makes the load-carrying structure which is responsible for providing the structural integrity necessary for the fuselage and the antenna PCBs are inserted individually in the load-carrying structure as shown in Fig. 1c.

3 Experimental results

The S-parameters and the embedded element patterns of the antenna array were measured at Chalmers anechoic chamber. The active reflection coefficients and the total radiation antenna patterns are obtained by post-processing the measured S-parameters and embedded element patterns respectively. The array is excited with uniform amplitude distribution and linear progression phase distribution for beam steering. Fig. 2a shows the active reflection coefficients (Γ_{act}) of the antenna array. The reflection coefficients are lower than the targeted level (i.e., 20% bandwidth) when steering up to ±60° whereas, at 75°, the bandwidth reduces to 10% due to the edge effects of our finite-sized array. Figs. 2b and 2c show the radiation patterns at 2.7 GHz at different azimuth angles and the realized gain over frequency at the broadside respectively. The simulations and measurements agree well. The array antenna has an efficiency of ≥80% within the targeted bandwidth (i.e., from 2.4 GHz to 3 GHz).

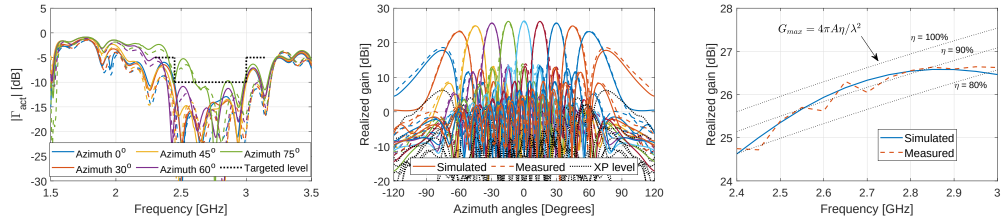

(a) Γ_{act} **(b)** Radiation patterns at 2.7 GHz **(c)** Realized gain at broadside

Figure 2. The 16×16 vertical bowtie element array when beam steering at different azimuth angles. (a) The active reflection coefficients and (b) the radiation patterns at 2.7 GHz. (c) The realized gain over frequency at broadside.

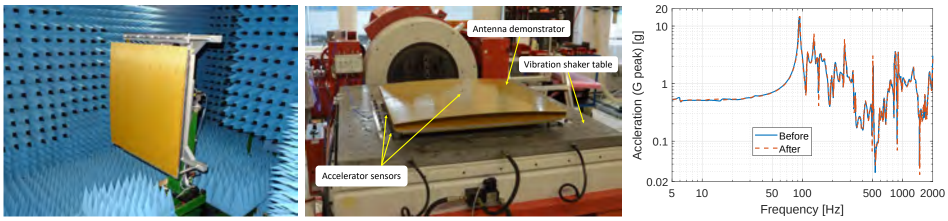

(a) Array at anechoic chamber **(b)** Array at vibration test rig **(c)** Dynamic response

Figure 3. Photo of (a) the array antenna and (b) the array at the vibration test rig. (c) Dynamic response of the array in a sinusoidal sweep before and after the vibration tests on one sensor location.

For the vibration test, the demonstrator was placed on a vibration shaker table with accelerometers at different locations in the demonstrator as shown in Fig. 3b. The vibration test levels were the same as those used in the vibration test of a typical commercial transport aircraft. Fig. 3c shows the dynamic response of the array demonstrator before and after the vibration tests on one accelerometer sensor location. The dynamic response before and after agree well, which indicates that there is no damage to the structure during the vibration test. The demonstrator was also inspected visually before and after the vibration test. There were neither loosened screws nor wear on the radome, ground plane as well as antenna PCBs. The peaks of the dynamic response indicate the natural resonance frequencies of the array demonstrator. The vibration test results show that the demonstrator has a low dynamic response, which indicates that the design concept is stiff.

4 Conclusion

A low-profile structurally fuselage integrated load-carrying array antenna is presented in the paper for wide beam steering application. The array is designed to fulfil the electrical requirements of an airborne antenna sensor as well as the mechanical requirements of a load-carrying aircraft fuselage. The 16×16 elements array demonstrator is capable of beam steering up to ±60° and ±75° with the bandwidth of 20% and 10% respectively at $\Gamma_{act} \leq -10$ dB. Various vibration loads equivalent to that of a commercial mid-range transport aircraft were used which established its natural frequency as well as tested its mechanical strength. The combination of the electrical and mechanical characteristics makes the proposed array antenna unique.

References

[1] M. H. Sadraey, *Design of Unmanned Aerial Systems*. A John Wiley & Sons, Inc Publication, 2020.

[2] J. Verpoorte et al., "Multifunctional structures to reduce the energy consumption of future aircraft with integrated ku-band antennas," *The Project Repository Journal (PRj)*, 2021.

[3] A. A. Fyall, "Practical aspects of rain erosion of aircraft and missiles," *Philosophical Transactions of the Royal Society of London. Series A, Mathematical and Physical Sciences*, 1966.

[4] M. Martínez-Vázquez et al., "Structurally integrated phased array antennas for aeronautical satcom applications," in *2021 15th European Conference on Antennas and Propagation (EuCAP)*, 2021.

[5] H. Qing-Qiang et al., "Research on structurally integrated phased array for wireless communications," *IEEE Access*, 2020.